Controllable release of vascular endothelial growth factor (VEGF) by wheel spinning alginate/silk fibroin fibers for wound healing

DOI:
10.1016/j.matdes.2021.110231

Document Version
Final published version

Journal Pre-proofs

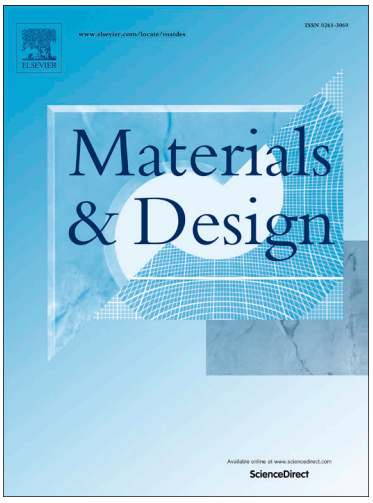

Controllable release of vascular endothelial growth factor (VEGF) by wheel spinning alginate/ silk fibroin fibers for wound healing

Jun Song, Zhongda Chen, Zekun Liu, Yangpeiqi Yi, Olga Tsigkou, Jiashen Li, Yi Li

PII: S0264-1275(21)00786-3
DOI: https://doi.org/10.1016/j.matdes.2021.110231
Reference: JMADE 110231

To appear in: *Materials & Design*

Received Date: 8 July 2021
Revised Date: 1 October 2021
Accepted Date: 7 November 2021

Please cite this article as: Song, J., Chen, Z., Liu, Z., Yi, Y., Tsigkou, O., Li, J., Li, Y., Controllable release of vascular endothelial growth factor (VEGF) by wheel spinning alginate/ silk fibroin fibers for wound healing, *Materials & Design* (2021), doi: https://doi.org/10.1016/j.matdes.2021.110231

Controllable release of vascular endothelial growth factor (VEGF) by wheel spinning alginate/ silk fibroin fibers for wound healing

Jun Song [a, 1], Zhongda Chen [a, 1]*, Zekun Liu [a], Yangpeiqi Yi [a], Olga Tsigkou [a], Jiashen Li [a], Yi Li [a]*

a Department of Materials, The University of Manchester, Manchester, M13 9PL, UK

1 These authors contributed equally to this work.

*Corresponding authors' emails:

zhongda.chen@postgrad.manchester.ac.uk,

henry.yili@manchester.ac.uk

Highlights:

- Wheel spinning technique was used to produce wet spun alginate composite fibers.
- Alginate/ silk fibroin morphologies and concentrations control vascular endothelial growth factor release.
- The design of experimental factors and interactions address release mechanisms.
- Non-linear fitting was introduced to describe vascular endothelial growth factor release behavior.

Abstract

The acute wound healing process requires a quick and short-stage vascular endothelial growth factor (VEGF) supply, especially, in the early-stage of injury. To date, research has rarely met the demand for controlled VEGF quick release. Herein, a novel wheel spinning technique was introduced to fabricate alginate (Alg)/ silk fibroin (SF) composite fiber for loading VEGF and achieving controllable release. In turn, it was demonstrated that the parameter of wheel spinning and Alg/SF material morphological combination significantly influence VEGF release behavior and fiber degradation speed, which could be controlled by adjusting spinning solution concentration and modifying SF morphology. The loading concentration and SF structural features interacted with each other to affect the VEGF release behavior, indicating that growth factors such as VEGF could be released in a controllable fashion. It could therefore be developed as a novel approach to control the wound healing process.

Graphic Abstract

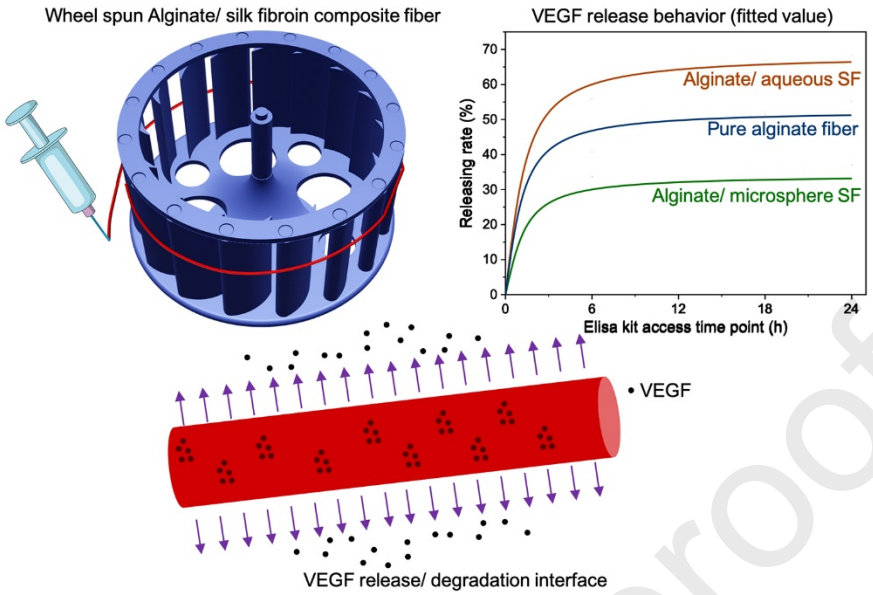

Key words: Composite fiber, wet spinning, alginate, silk fibroin, growth factor, design of experiment

1. Introduction

Human skin wound healing, especially for acute wound, is a phased process involving the contribution of varieties of growth factors and cytokines [1,2]. After neutrophils gathered on the wound interface through blood capillaries in minutes, monocytes and lymphocytes arrived within the next few hours [3]. These cell lineages not only defended against contaminations, but were also sources of growth factors [4]. VEGF is one of the essential growth factors in the early stages of acute wound healing necessary to achieve the proliferation of capillaries in the granulation tissue, so as to accelerate the rate of reendothelialization within a few minutes or hours [5,6].

Bioactive wound dressing is one of the clinical options available during the wound healing process, including multiple functions [7,8], i.e., enhancing an anti-inflammatory environment, maintaining cell adhesion and elevating cell proliferation, and loading and releasing growth factors. Natural polysaccharides and polypeptides are mainstream biodegradable and biocompatible wound healing materials with low immune response [9]. Next-generation wound healing systems should be able to maintain therapeutic levels of growth factor on a wounded interface desirable speed and volume [10]. As one of the cutting-edge commercial wound healing systems, the nonwoven macromolecule composite dressing has a three-dimensional cross-linked porous network which can absorb up to tens of times the dry weight of water [11].

Wet spinning is a historic and generic composite fiber manufacturing technology, in which a polymer solution is pumped through tiny holes of a spinneret under pressure into a coagulation bath until it reaches a critical concentration, after which it coagulates and solidifies into fibers [12]. However, a solution of high concentration ions and high temperature have typically led to protein denaturation and growth factor deactivation [13]. Involving another natural macromolecular to

optimize wet spun composite fiber is an alternative strategy [14]. Extracted from seaweeds, alginate is a biocompatible, biodegradable and renewable wound healing material approved by the United States Food and Drug Administration and its counterparts globally [15,16]. Furthermore, alginate has shown the potential to be wet spun under a low-temperature and low-concentration calcium chloride coagulation bath to maintain the bioactivity of VEGF, which promotes wound angiogenesis [17]. Either silk fibroin aqueous solution or microspheres can be mixed with alginate spinning solution [18,19]. Notably, human wound exudate contains sodium ions while calcium alginate contains calcium ions. When applying calcium alginate wound dressing onto the wound interface, the calcium ions exchange sodium ions, such that the dressing generates a gel area on the wound surface in order to provide a barrier against invading microorganisms.

In this article, we hypothesize that the wet spun Alg/SF composite fiber loaded VEGF can achieve the controlled quick release of VEGF and stable low-speed degradation for wound healing applications. We further hypothesize that silk fibroin formations and wet spinning parameters may influence physical properties, biodegradability, and the growth factor release speed of composite fibers. Therefore, three kinds of Alg or Alg/SF based composite fibers were fabricated by a novel wheel spinning technique under conditions involving a low-concentration coagulation bath at room temperature. The mechanisms of composite fiber fabrication were introduced. The VEGF was directly loaded into the spinning solutions for the application of wound healing dressing loaded growth factors. The experimental results and DoE effects of VEGF release performances were studied in Minitab with *in vitro* evaluation evidencing our hypothesis.

2. Materials and methods

2.1 Materials

The procurement of raw *Bombyx mori* silk was from Shengzhou Xiehe Silk, Zhejiang, P. R. China. Sodium alginate (Alg) powder (W201502) and lithium bromide (LiBr) were purchased from Sigma Aldrich, USA, and used without further purification. Ammonium sulfate ($(NH_4)_2SO_4$), calcium chloride ($CaCl_2$), and sodium carbonate (Na_2CO_3) were purchased from Fisher, UK.

2.2 Regenerated silk fibroin solution and microsphere preparation

Silk fibroin was dissolved using lithium bromide solution [20]. Natural *Bombyx mori* silk was degummed in a boiling 0.02 M Na_2CO_3 aqueous solution. The degummed silk was dissolved by 9.3 M LiBr aqueous solution at 60℃ for 4 h. Cellulose semi-permeable membranes (molecular weight cut-off 12,000-14,000, SERVAPOR, Germany) were applied in order to dialysis subject the dissolved high-concentration silk fibroin/LiBr solution to dialysis. The regenerated silk fibroin solution at around 6.8 wt% was filtrated and centrifuged twice before further processing.

The regenerated SF microspheres were prepared via wheel spinning, which is a modified wet spinning technique. Similar to the traditional wet spinning technique, 3 wt% regenerated SF solution was ejected into an ammonium sulfate coagulation bath (25 wt%) at 25°C. Upon completion of the wheel spinning process, the SF/$(NH_4)_2SO_4$ solution was left stand for 1 h to collect SF microsphere sediments. After washing softly using deionized water for removing ammonium sulfate, the SF microspheres were consequently transferred to a refrigerator at -20°C

for 24 h. It was then possible to collect the dry particulate regenerated SF after an overnight lyophilizing.

2.3 Alginate/silk fibroin fiber fabrication

The designed wheel spinning device was used to prepare Alg and Alg/SF fibers [21]. As Figure 1b demonstrates, three kinds of Alg or Alg/SF wet spinning solution were extruded into a calcium chloride coagulation bath at a speed of 1 ml/min by means of a 30G needle. The wheel spun rotational speed was 200 rpm/min. For Alg/SF samples, the silk fibroin, which would either be regenerated microspheres or aqueous solution, was mixed with alginate solution at a certain ratio. The design of experiment for composite fibers is presented in Table 1.

For growth factor loading specimens, the recombinant human vascular endothelial growth factor (VEGF-165, Generon, UK) was added into Alg and Alg/SF solution before spinning (Figure 1a). The concentration of growth factor added during spinning was fixed at 6.75 ng/mg for all sample groups. However, it was inevitable that growth factor would deplete during wheel spinning and further processing. Hence, the final actual loading amount was less than 6.75 ng/mg in this work. The loading efficiency is discussed in the result sections.

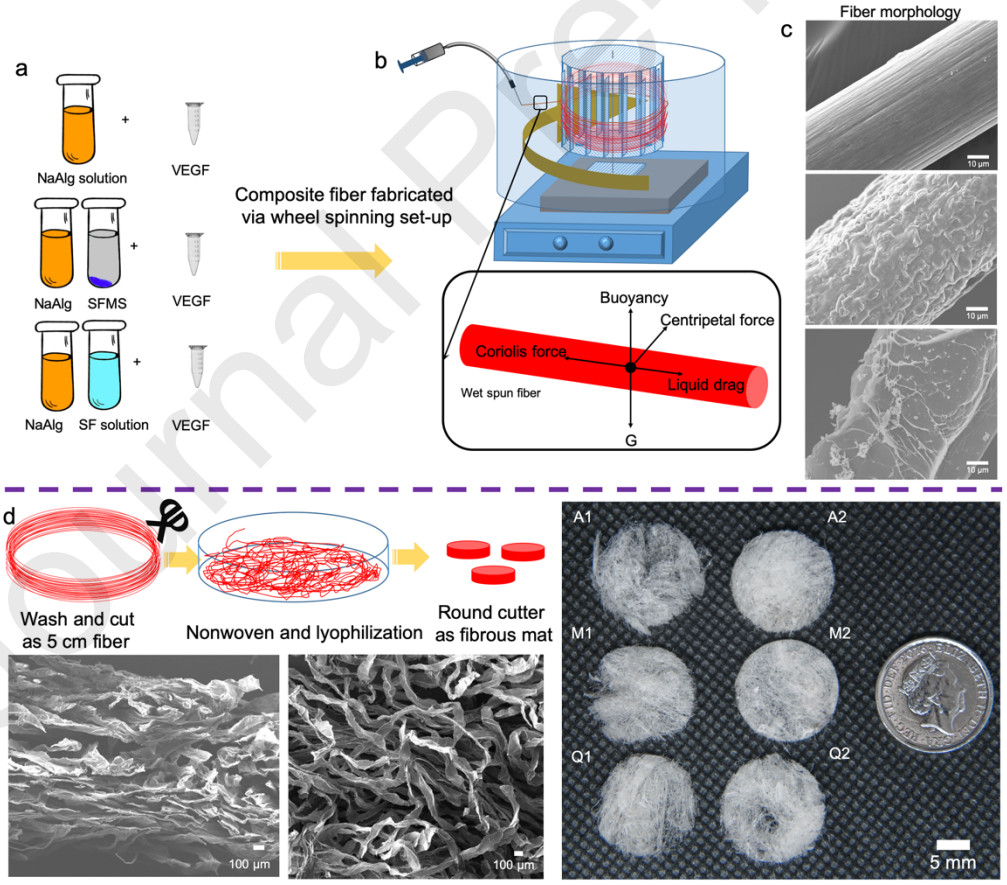

Figure 1. (a, b) Wheel spinning schematic to fabricate alginate/silk fibroin fibers; (c) surface morphology of composite fibers; (d) schematic and surface morphology of alginate/silk nonwoven

composite fiber.

2.4 Alginate/fibroin nonwoven fabrication

The acquired wheel spun fibers were washed softly and chopped into 5 cm short threads. As Table 1 shows, six sample groups were set, based on different Alg/SF concentrations and silk fibroin formations. The pure alginate samples were marked as A1 for 1 wt% Alg concentration and A2 for 3 wt% concentration. The sample groups containing microsphere or aqueous silk fibroin were marked as M1 (1 wt% Alg / microsphere SF), M2 (3 wt% Alg / microsphere SF), Q1 (1 wt% Alg / aqueous SF) and Q2 (3 wt% Alg / aqueous SF), respectively. The chopped short Alg or Alg/SF fibers were dispersed and formed as nonwoven composite mats in wet condition. The nonwoven fibrous composite mats were lyophilized at -40℃ until thoroughly dry.

Table 1. Design of experiment for production of wheel spun alginate/ silk fibroin fibers.

Sample ID	Concentration $C_{Alg}+C_{SF}$		SF formation
	Alg concentration (wt%)	SF concentration (wt%)	
A1	1	0	N/A
A2	3	0	N/A
M1	0.5	0.5	Microsphere
M2	1.5	1.5	Microsphere
Q1	0.5	0.5	Aqueous
Q2	1.5	1.5	Aqueous

2.5 Fiber and composite characterizations

The surface morphology of Alg or Alg/SF fibers and nonwoven composite mats were observed by means of a field emission scanning electron microscopy (FE-SEM, Zeiss Ultra 55, Germany) at 1.5 kV after gold coating. Both fiber and nonwoven composite specimens were frozen sectioned in a cryostat (CM3050s, Leica Biosystem, UK) in order to observe cross-section morphology by Ultra 55.

For characterizing the difference between two kinds of Alg/SF fibers, the dried SF membrane, chopped Alg, and two kinds of Alg/SF fibers were mixed with potassium bromide powder and pressed into plates for Fourier transform infrared (FTIR) characterization using a Nicolet 5700 spectrophotometer (Thermo, USA) in transmittance mode.

X-ray diffraction (XRD) of dried pure SF membrane, chopped Alg and two kinds of Alg/SF fibers were scanned to investigate crystallization by using an X'Pert Pro's X-ray diffractometer (Panalytical, UK) with reflection mode Cu-Kα radiation operated at a voltage of 40 kV and a filament current of 40 mA, employing a scanning rate of 2°/min in a 2θ range from 5° to 50°. The mechanical properties of the chopped dry wheel spun fibers (25 mm) were performed by a universal materials tester (Instron 5566, MA USA) at a crosshead speed of 2 mm/min.

2.6 *In vitro* degradation

Nonwoven composite sample degradation behavior was determined by a temperature-controlled water bath shaker, set at a shaken rate of 55 times/ min and 33℃, to simulate a wound surface environment. Weight loss on day 1, day 7, and day 14 was calculated by the following Equation (1).

$$R_{\text{weight loss}} = \left(\frac{w_0 - w_t}{w_0}\right) \times 100\%, \quad (1)$$

where w_t is the weight of the nonwoven composite sample after the degradation test, and w_0 is the weight of the pristine sample before the degradation test.

Silk fibroin degradation behavior was traced via the Pierce™ Coomassie Plus (Bradford, Fisher, UK) assay kit, which can detect the concentration of SF in soaked medium and calculate the remaining SF volume within the fiber. Thus, it was possible to obtain the SF degradation rate via the following Equation (2).

$$R_{\text{SF}} = \frac{W_{SF} - C_b \times 1ml}{W_{SF}} \times 100\%, \quad (2)$$

where C_b is the concentration measured by the Bradford assay, and W_{SF} is the SF weight pristine nonwoven composite sample.

2.7 Measurement of VEGF release from alginate / silk fibroin composite fibers

The release of VEGF took place in a 24-well plate, with 1 ml of DMEM added into each well. Human VEGF enzyme-linked immunosorbent assay (ELISA) kits were purchased and assayed at four time points (1, 6, 18 and 24 h), according to the manufacturer's instruction (Bio-Techne, USA). To minimize the pipette operating impacts on the release of growth factor, each individual specimen was only used for collecting one set of time point data.

2.8 Statistics

Fiber degradation, cell work and VEGF releasing analysis were performed using IBM SPSS (version 24.000). These data were expressed in terms of mean ± standard deviation. A one-way ANOVA test was used to evaluate intergroup differences, and a p-value of <0.001 was considered statistically significant and presented as (*) in figures. The VEGF loading efficiency, VEGF release rate and Alg/SF fiber weight loss were graphed and analyzed using Minitab 17 (Minitab, LLC) and MATLAB 2018 (MathWorks, Inc) in order to reveal the relationship between the results and DoE factors [22].

3. Results and discussion

3.1 Alginate/silk fibroin fiber and composite fibers

3.1.1 Wheel spun alginate/silk fibroin fiber

Wet spinning is considered as a traditional chemical fiber manufacturing method, which can process regenerated polysaccharides or polypeptides, i.e., alginate or silk fibroin fibers. Some post-treatment steps such as stretching or finishing were applied to modify wet spun fibers. Instant and *in situ* treatment of wet spun fibers in a coagulation bath can also improve fiber quality as well as having been known to change scientists' and engineers' impression concerning the low-production

efficiency of wet spinning technology.

Compared with synthesis polymers, the fabrication of natural polysaccharides and polypeptides are more facile, eco-friendly, economical and easy to production on a massive scale. Silk fiber has been applied as wound healing material, such as in surgical sutures several long decades [23]. Owing to the degumming treatment undertaken to remove sericin, the regenerated silk fibroin, a typical polypeptide, can avoid inflammation, which explains its use as a wound healing material [24]. Benefiting from a facile fabrication method, flexible structure, and adjustable physical and chemical properties, composite fibers can be functionalized by loading growth factor onto bioactive wound healing dressings. Wet spinning technology applies the liquid coagulation bath to solidification polymer solution. Some researchers have reported regenerated SF fibers can be prepared via wet spinning with ammonium sulfate or an organic solvent coagulation bath [25,26], which would severely break the molecular chain of fibroin and decrease its physical properties [27]. By involving a novel wheel spinning set-up, this project introduced a unique wheel spinning set up. As Figure 1b demonstrates, an Alg/SF polymer solution jet from the needle solidified and rolled on the rotator. This design reduced the size of the whole set up and elevated the efficiency of fiber collection. Figure 1b also presents the force analysis for wheel spun fiber in the $CaCl_2$ coagulation bath. Upon a solution jet of alginate or a mixture of alginate and silk fibroin being injected into the coagulation bath from the needle, the vertical buoyancy and gravity made the fiber stable in the bath. The injected solution was then quickly coagulated towards a hydrogel fiber due to the chemical reaction between alginic acid and calcium chloride. As the fiber slowly approached the center of the bath vat, the vortical rotator applied a Coriolis force and a tangential centripetal force to the fiber [28]. Coriolis and centripetal forces can lead to polymer fiber deformation. The direction of the Coriolis force was opposite to the liquid drag of fiber. The simulations on polymer solution which applied a Coriolis force were mainly focused on spinning coating fabrication [29]. A specific theorical model for wet spinning solution or similar polymer jets, when applying a Coriolis force, is neither established nor well acknowledged. Thus far, it can only be confirmed that polymer viscoelasticity is the key factor influencing fiber diameter and mechanical performances [30].

3.1.2 Surface morphology and mechanism of alginate/silk fibroin composite fibers

The continuous and robust surface morphology was another advantage of this wheel spinning set-up. It can be seen in Figure 1c that both Alg and Alg/SF fiber had a uniform fiber surface and diameter (Figure S1). The pure alginate fiber was smooth, while two kinds of Alg/SF composite fiber revealed a wrinkled rough surface. There were also some highly oriented grooves on the pure alginate fiber. Figure 2b demonstrates the chemical reaction between the sodium alginate spinning solution and the calcium chloride coagulation bath, which contributed to this oriented groove morphology. Specifically, when the alginate spinning solution was rapidly squeezed into the coagulation bath, the calcium ions' cross-linked alginate molecular chains went onto form lateral egg-box complex dimers (Figure S2) on the spinning solution / coagulation bath interface [31]. These cross-linked alginate molecular chains were further agglomerated towards robust alginate nanospheres (Figure S3) as indicated in the cross-section SEM image of alginate fiber in Figure 2a [32]. In turn, the shear force from the needle of the spinning set-up led alginate nanospheres towards

the oriented grooves.

In fact, most researchers in bio-materials have used lyophilized SF powder as a raw material [33]. In this work, the SF microsphere (SEMs in Figure S4) was cross-linked through ammonium sulfate, then freeze-dried. However, this SF microsphere cannot be regarded in terms of typical lyophilisomes. Regenerated SF is a fibrils polypeptide, which is extremely sensitive to ions solution and facilitates conformational transition. As for ammonium sulfate, previous studies have reported the successful fabrication of a SF microporous membrane or wet spun fibers [34]. Combined with related reports, it was confirmed that a lower-concentration ion coagulation bath cannot transit SF conformation and orientate the SF molecule chains. Thus, the optimized wheel spinning set up was able to scatter the SF jet flow to microspheres. Combined with the alginate agglomerated egg-box multimers fabricated by wheel spun in the previous study [21], SF influenced the alginate aggregation when these either aqueous or microspheres SF microspheres were mixed with alginate spinning solution and wheel spun again as Figure 2b shown. As an improvement of conventional chemical engineering technology, wheel spinning set-up tries to fill the gap between macro materials and molecular level substances [35]. The SEM images in Figure 2a present the cross-section of Alg/SF microsphere composite fiber. It is critical that the calcium chloride used for alginate spinning also preserved SF as a nanofibril, in other words, in a random-coil state [36]. As the cross-section SEM image of Alg/SF aqueous composite fiber in Figure 2a confirms, the SF nanofibril self-assembled into nanoparticles, became attached to the alginate and spun into composite fibers.

Tensile tests

3.2 Composite fiber wound healing material characterization

FTIR spectroscopy was conducted to investigate the different secondary structures of alginate and fibroin in three kinds of fiber specimens. In general, the FTIR curves of the two kinds of Alg/SF hybrid fibers were significantly different (Figure 2c). The fiber fabricated by alginate and SF microspheres was more similar to pure alginate fiber, while the fiber fabricated by alginate and aqueous SF was akin to pure SF specimens. In the case of Amide I and Amide II regions of SF, previous literatures has indicated that typical characteristic peaks at ~1655 cm^{-1} and ~1540 cm^{-1} refer to the random coil conformation of peptide, while the characteristic peaks at ~1630 cm^{-1} and ~1520 cm^{-1} are characteristic indicate β-sheet conformation, respectively. The characteristic peak of Amide II was observed in fibers containing either microsphere or aqueous formation SF. However, the aqueous SF fiber remained as random coil in Alg/SF fiber, whereas the SF microsphere were subject to β-sheet conformation, resulting in a more stable state of fibroin. The Amide I adsorption peak of SF could only be observed in Alg/SF aqueous fiber. Conversely, the asymmetric band, i.e., the intense stretching vibration peak at 1600 cm^{-1}, of carboxylate anions could only be observed in pure alginate and Alg/ SF microsphere fibers. As the dotted box in the figure shows, the peaks at 1410 cm^{-1} were assigned to the symmetric band of alginate, which could be detected in all three kinds of fibers. FTIR curves proved either microsphere SF or aqueous SF was successfully spun with alginate into fibers. The microsphere formation of SF was more stable than the aqueous formation of SF in Alg/SF fibers.

XRD for three kinds of fibers was also conducted, and the relevant patterns are introduced in Figure 2d. All three fibers retained a low crystalline state. This is reasonable due to these two natural polymers not being crystallized during processing. A diffraction peak at around 13.4° could be observed in Alg or two Alg/SF fibers. This peak should be assigned to the lateral packing among alginate molecular chains. The Alg/SF microsphere specimen had a relative intensive peak at 20.7°, which was a typical diffraction peak for the Silk II state. According to the cross validation carried out using infrared spectroscopy, the demonstrated results of XRD are consistent with those of FTIR.

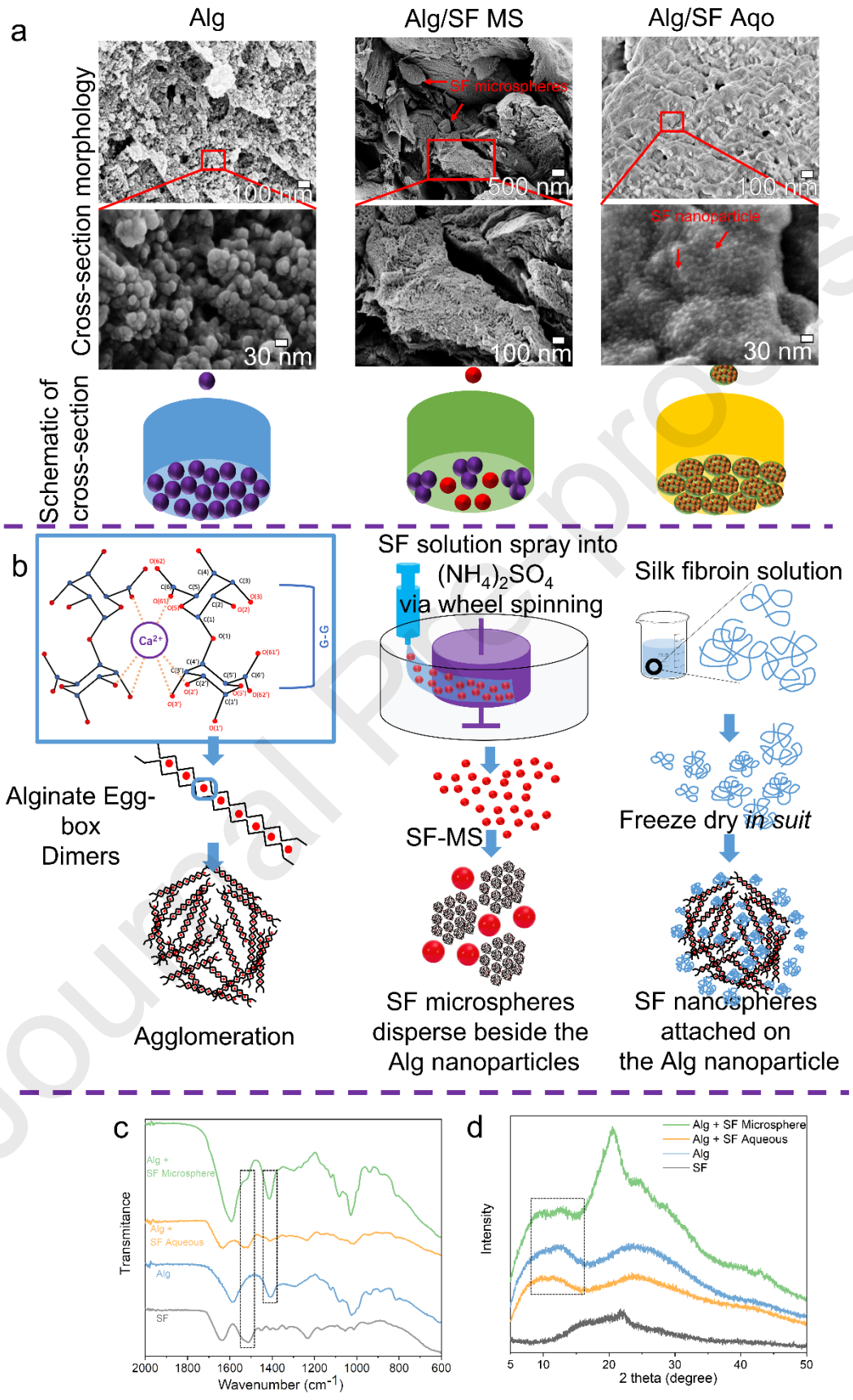
a
Alg
Alg/SF MS
Alg/SF Aqo
Cross-section morphology
SF microspheres
SF nanoparticle
100 nm
500 nm
30 nm
Schematic of cross-section
b
SF solution spray into
$(NH_4)_2SO_4$
via wheel spinning
Silk fibroin solution
Alginate Egg-box Dimers
SF-MS
Freeze dry *in suit*
Agglomeration
SF microspheres disperse beside the Alg nanoparticles
SF nanospheres attached on the Alg nanoparticle
c
Alg + SF Microsphere
Alg + SF Aqueous
Alg
SF
Transmitance
Wavenumber (cm^{-1})
d
Alg + SF Microsphere
Alg + SF Aqueous
Alg
SF
Intensity
2 theta (degree)

Figure 2. (a) The cross-section surface morphology of three kinds of Alg/SF fibers. (b) The alginate reacts in a calcium chloride coagulation bath to form lateral egg-box complex dimers at the spinning solution / coagulation bath interface. SF spinning solution jet flow was broken by the optimized wheel spinning set-up to microspheres. The aqueous SF was kept in a random-coil state and attached to the alginate, then spun into composite fibers. FTIR patterns (c) and XRD curves (d) of Alg/SF microsphere (green), Alg/SF aqueous (yellow), pure alginate composite fiber (blue) and pure silk fibroin microsphere (black) specimens.

3.3 Alginate/ silk fibroin composite fiber loaded VEGF

Traditional breathable, waterproof and topologically structured wound dressing could only meet the basic criteria of biocompatibility. In recent years, striking a balance between physical structure and bioactivity for wound healing materials has been a hot topic. Table 2 presents some of the parameters from previous work into different formats of alginate or silk fibroin materials which loaded VEGF onto bioengineered scaffolds. Most researchers report on growth factor loading amounts and releasing volumes at certain time points throughout the day. However, standard examination criteria have yet to be established concerning the releasing performances of growth factors. At present, there are only a few studies which critically review or present research on growth factor loading efficiency [37]. To this extent, Table 2 reviews and calculates VEGF loading efficiency and releasing speed based on data collected in the literature. Some researchers have reported relatively high loading efficiency in case of chemical conjugation [38]. However, the release rate of growth factors loaded by chemical methodology was difficult to control. Thus, it was only suitable for chronic wounds which need a slow release over a period of weeks. In this study, by controlling the degradation rate of alginate and silk fibroin, VEGF was loaded by using a physical method in order to achieve controllable quick release alongside slow degradation composite fibers. As the SEM images Figure 2 demonstrated, three groups of Alg or Alg/SF fibers had different mesoscale morphology with each other due to the wheel spinning method. These morphological differences provide the possibility to achieve the controlled release of VEGF.

Figure 3 demonstrates the evaluation protocols for VEGF loading efficiency. VEGF loading efficiency was calculated by measuring the VEGF concentration that was lost in the coagulation bath using ELISA assay kits. Based on the interval plot in Figure 3b, d and consequent main effect results Figure S5, there was no significant difference in VEGF loading efficiency among three kinds of composite fibers. The Alg/SF microsphere composite fiber had the worst VEGF loading rate. The higher-concentration sample usually enjoyed a slightly better loading rate than that the lower-concentration sample for the same Alg/SF composite fiber.

Table 2. Pervious reported VEGF releasing parameters for alginate or SF based scaffolds.

Alginate or SF based scaffolds	Time point (day)	Loading amount (ng/mg)	Loading efficiency (%)	Release ratio (%)	Release speed (%/day)	Ref
Silk fibroin core-shell electrospinning	1, 2, 4, 7, 10,	0.28, 0.58	33-67%	7%, 11%	2.5, 7.5	[39]

Vancomycin/ Silk nanoparticle	13, 16 1, 3, 7, 14, 21, 28	10	97%	14%	0.7	[40]
Silk fibroin/ calcium phosphate/ PLGA nanocomposite	1, 3, 7, 14, 28	4	65%	6%	0.8	[41]
Wheel spun Alg/SF composite fiber ★ this work	Within 1 day	6.75	30%	9-22%	25-70	★
Injectable alginate composite hydrogel	1, 3, 5, 7, 14,	11800	N/A	51%	26	[42]
Hybrid Polycaprolactone/Alginate Scaffold	0 - 14	350	61-77%	5%	4.5	[43]
VEGF-conjugated alginate hydrogel	1, 3, 7, 14, 28	4.1	14-16%	4%, 15%	0.1	[38]
Alginate/laponite hydrogel microspheres	0, 3, 7, 14, 28	10	45%	11- 16%	1.5-2.3	[44]

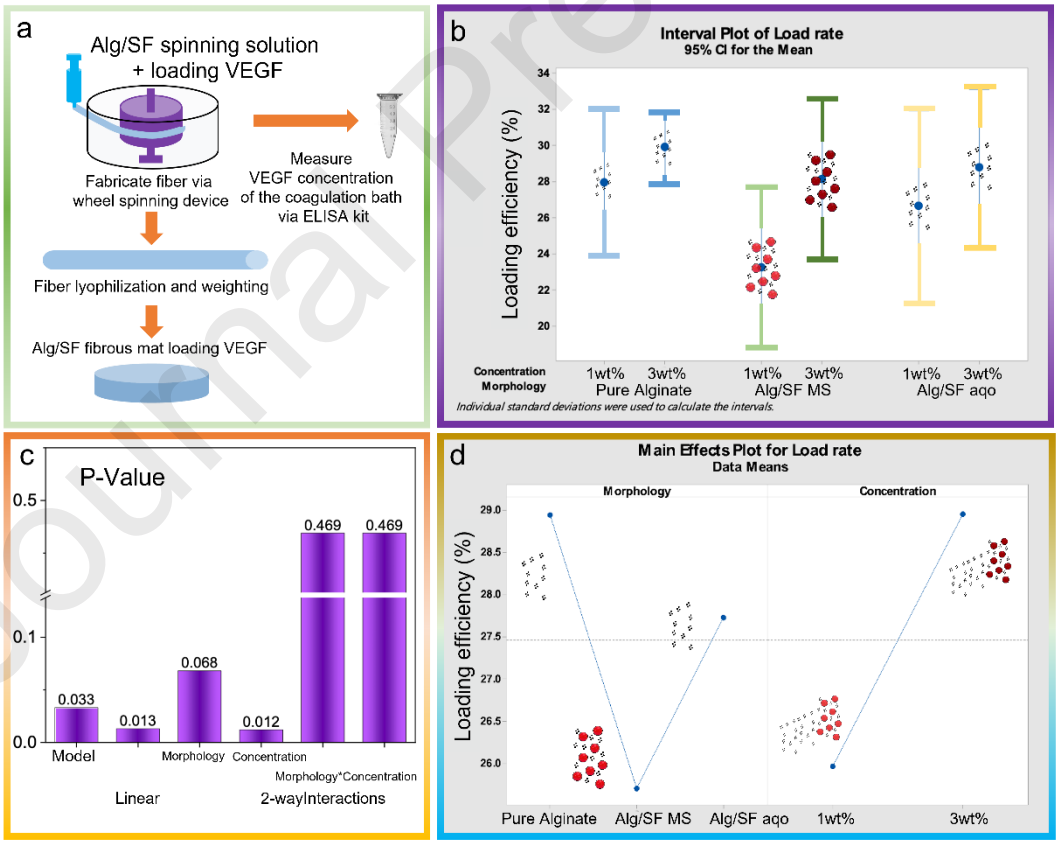

Figure 3. VEGF loading efficiency was calculated by measuring VEGF concentration lost in the coagulation bath by using ELISA assay kits. (a) Measurement schematic for VEGF loading

efficiency, (b) the results of loading efficiency affect via DoE parameters, main effect (c) P-Value and (d) plot of VEGF loading efficiency in Alg/SF composite fibers.

3.4 Controlled release of VEGF via silk fibroin inside alginate fiber

The 24-h release kinetics of VEGF loaded by Alg/SF composite fibers was measured by using ELISA assay kits at four time points, as exhibited in Figure 4. The Figure 4a demonstrated the evaluation protocols for VEGF releasing rate and speed. VEGF releasing speed could be defined as the quotient of the growth factor quantity released and time in a given period. Thanks to the calcium alginate formed during the wet spinning on fibers' surface, the Alg/SF fibers in this work can remain relatively stable in water or air environments. On the contrary, once the fiber or non-woven structure touches the human wound interface, sodium/calcium ions exchange would occur, and the release of VEGF will begin. This situation can essentially be understood as a trigger mechanism. The physical loading method in this study followed the characteristics of an arctangent function image. Specifically, a large proportion (30%) of VEGF was released within 24 h. The VEGF release rate calculation time of this study was within one day, whereas the release tendency and release volume were similar to those of other studies, i.e., from half to one month. A large proportion of VEGF was released in the first hour, which could be defined as quick release.

Developing theoretical models for describing growth factor release mechanisms has received considerable attention in recent years [45]. A arctangent function in Equation (3) was selected for nonlinear fitting in order to conclude the potential principle in this study [46].

$$y = A \times \arctan\left(B \times x\right), \quad (3)$$

This function was highly simplified, but effective as shown in Figure 4b. The *Coefficients A* represented the VEGF final release volume and confirmed the asymptote (y = A×pi/2) in the functions graph, while the *Coefficients B* represented the initial VEGF release speed and the fractality degree in graph of functions.

Upon alginate fiber immersion into DMEM, the cross-linked calcium alginate on the fibers' surface was converted into soluble sodium alginate, while VEGF was released alongside the dissolution of composite fibers. It was also observed that the VEGF release rate and the composite fiber degradation rate were essentially consistent. Comparing the Alg/SF fibers with alginate ones, the addition of SF aqueous solution increased the release rate and reduced the degradation rate. These changes may be attributable to soluble SF in the fiber. Aqueous SF is known to improve fluidity inside the hydrogel, making it easier for VEGF to effuse from Alg/SF aqueous composite fibers. The addition of SF reduced the relative concentration of alginate spinning solution. Thus, it was inevitable that the degradation rate would be lower than that of alginate fibers. Different from the SF aqueous, the addition of microspheres reduced both degradation speed and release rate at the same time. These changes may be due to the gaps between the interior SF microspheres and alginate, which made it difficult fo the composite fibers to disintegrate quickly after absorbing water. The alginate and SF concentration also affected the density of the fibers, as proven by the fiber diameter data in Figure S1. The alginate fiber was released quickly at a high concentration and degraded quickly, while the fiber of the Alg/SF microspheres released quickly at a low concentration and degraded quickly. Only Alg/SF aqueous fiber at a high concentration was released quickly and

degraded slowly. In conclusion, the addition of two kinds of SF had positive effects on composite degradation and VEGF releasing performances.

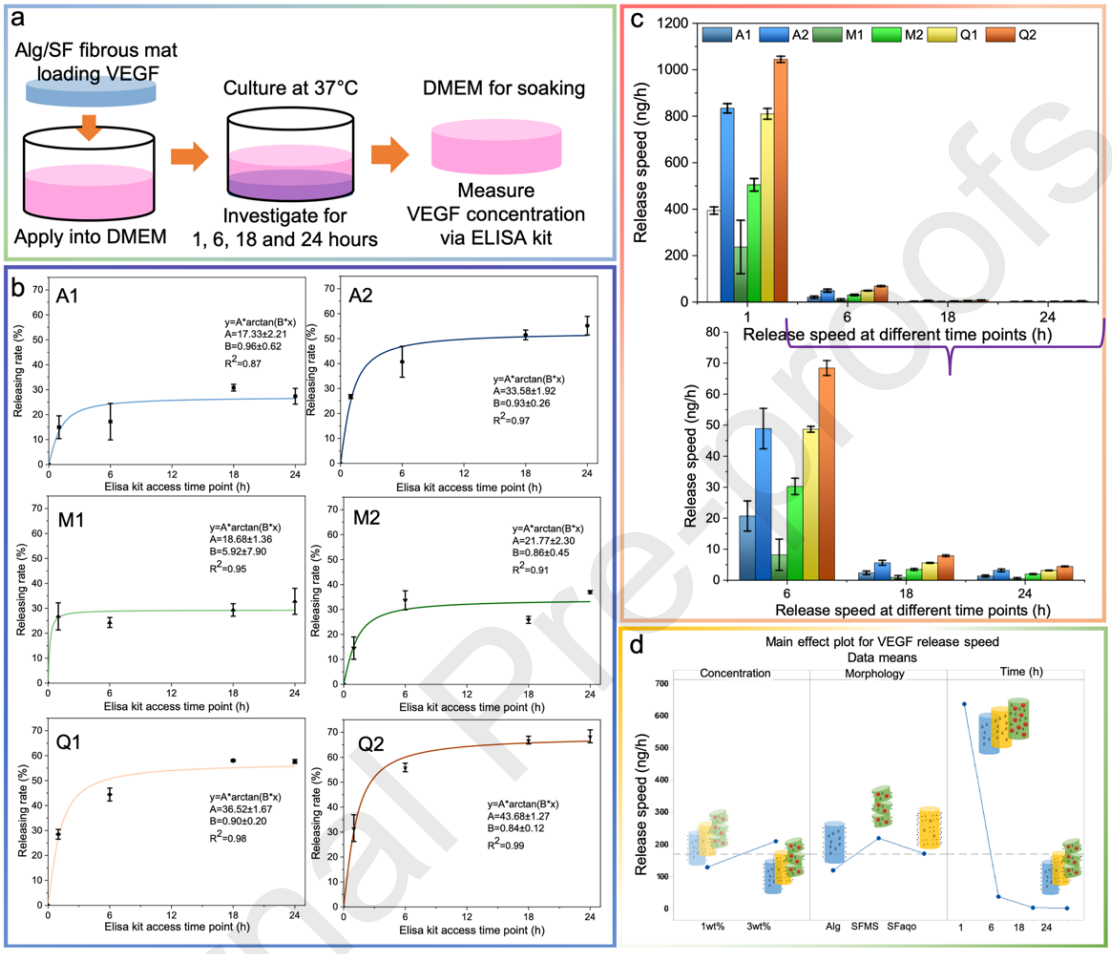

Figure 4. VEGF release behavior from Alg/SF composite fiber. (a) VEGF release rate scatter diagram and non-linear fitting curves for six groups of Alg/SF composite fiber. The VEGF releasing rate was calculated by measuring VEGF concentration in composite fiber soaked in DMEM solutions using ELISA assay kits at four time points. (b) Schematic diagram and (c) release speed for evaluating VEGF release performances. The VEGF release speed was calculated by measuring the first-order derivative of non-linear fitting curves and transferred to the actual amount.

3.5 Effect of silk fibroin morphology and spinning solution concentration

Based on the DoE presented in Table 1, Alg/SF composite fiber morphology and spinning solution concentration can affect VEGF release tendency and composite fiber degradation performance. As Figure 5a demonstrates, composite fiber morphology and concentration can affect weight loss significantly. Based on the evaluation of composite fiber VEGF release, it can also be confirmed that fiber morphology and concentration can affect release significantly. The addition of SF

microspheres reduced the release speed slightly, whereas the addition of aqueous SF increased the release speed sharply. Higher wheel spinning solution concentration caused a higher release rate, but the addition of SF microspheres weakened the effect. In the first hour of evaluating VEGF release, the spinning solution concentration did not affect the release too much.

Although our wound healing materials experienced slow degradation and quick VEGF release performances, it should be noted that excessively applying of VEGF, especially over a short period, causes edema or other complications [47]. Regarding the diversity and complexity of human wounds, the desired VEGF volume should be diverse too [48]. Our wound healing composite fibers can be adjusted by loading volume and comprise a mix of different kinds of fibers to ensure the quick release of necessary VEGF.

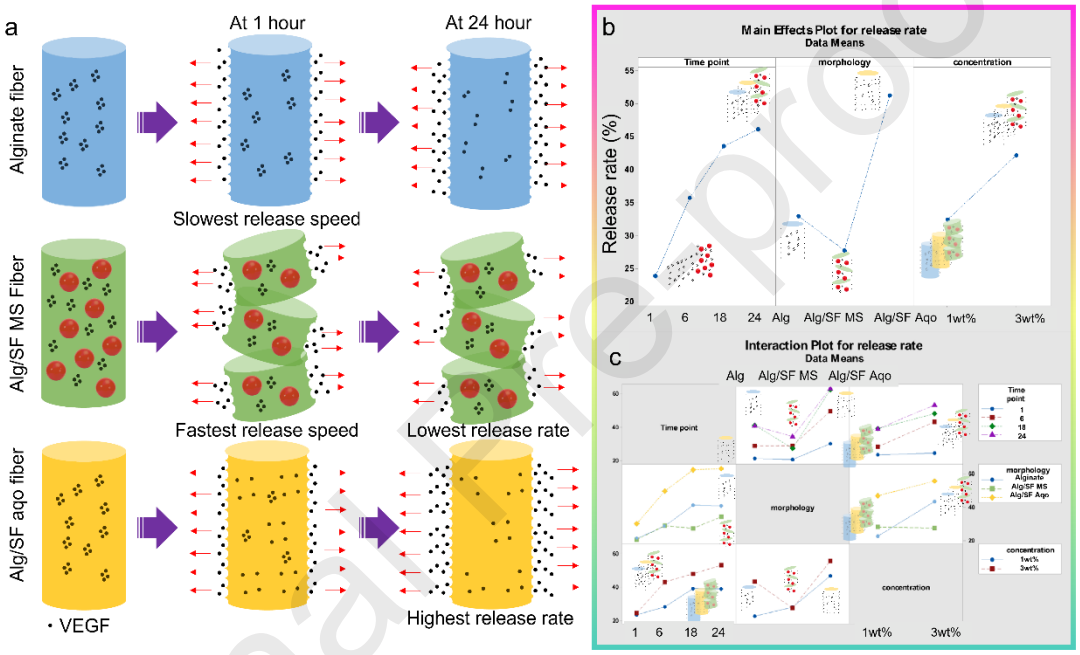

Figure 5. (a) Main DoE effect plot for Alg/SF composite fiber release rate, (b) interaction effect plot.

3.6 *In vitro* degradation evaluation for alginate/silk fibroin composite fiber

For the purpose of evaluating *in vitro* degradation performances, the samples were incubated in DMEM solution which mimics the human interstitial fluid in order to measure the quantitative changes. The schematic diagram in Figure 6a demonstrates the degradation study for Alg/SF composite fibers. The addition of either microsphere or aqueous SF reduced the level of weight loss while evaluating degradability, especially between the SF aqueous groups. The higher concentration fibers displayed a slower degradation speed, although it was faster in the first hour (Figure S6). It was found that the specimens of Alg/SF microsphere groups degraded faster than those of Alg/SF aqueous groups although the SF microspheres were cross-linked and more stable than in the SF aqueous groups. This was due to the insoluble SF microspheres in the fibers acting as they disintegrate. Further, the microscale SF ingredient indeed accelerated the breakdown of

composite fibers. However, after the SF microsphere brought about disintegration, the Alg/SF microsphere composite fibers experienced a slower degradation speed than the Alg/SF aqueous fibers. Comparing the degradation performances of three kinds of fibers, the pure alginate fiber quickly degraded at the beginning while the two kinds of Alg/SF hybrid fibers exhibited a relatively steady degradation performance during the 24-h-long evaluation. Furthermore, the Bradford assay was performed and the specific SF weight loss and degradation share were calculated for Alg/SF aqueous group. The vertical axis in Figure 5c represents SF degradation according to a logarithmic scale. It was obvious that the aqueous SF in composite fibers quickly degraded (500-550 μg) in the first hour of the experiment whereas alginate slowly degraded in the hours that followed.

Due to the SF and alginate are both acknowledged implantation materials with good biocompatibility [16,49], we believe the cell work to prove the basic *in vitro* cell viability is not necessary. However, the cell adhesion results are presented in the supporting information (Figure S12 & S13) because undue cell adhesion performances should be regraded a passive characteristic for wound healing materials.

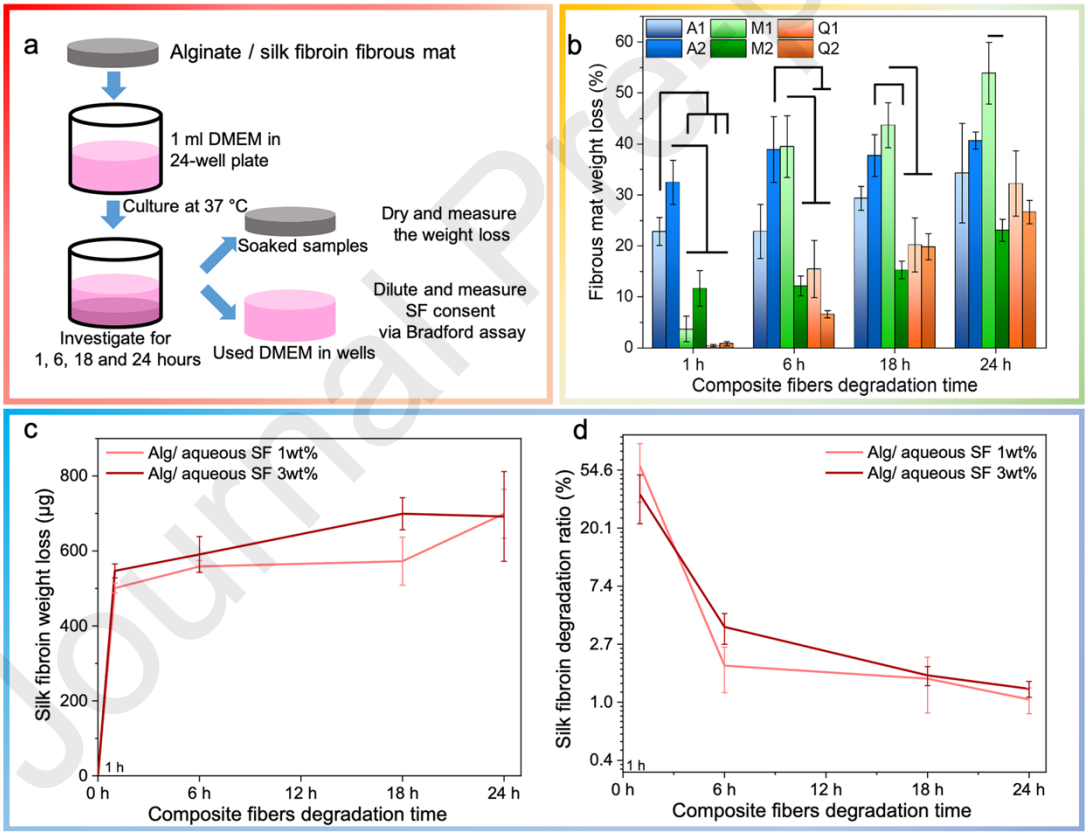

Figure 6. (a) Schematic diagram and (b) weight loss results for the composite fiber biodegradability study. The weight loss among composite fibers was investigated by drying and measuring samples soaked at four time points. The DMEM used in wells was diluted SF consent measured via the Bradford assay. (c) SF weight loss and (d) degradation ratio was consequently calculated and

presented.

3.7 How wheel spinning set-up affects physical properties of Alg/SF fibers

Based on the DoE study (Figure S7 - S11) of Alg/SF wheel spun fibers, the wheel rotation speed does affect the mechanical properties of wheel spun fibers as Figure 7 shown. The fibers' stain and stress show opposite changes with the speed of the three formulas of fibers increasing. For pure alginate fibers, the drawing rate of fibers becomes higher due to higher shear force from the coagulation bath flow, when the rotation speed increases. As the result, the pure alginate fabricated by higher rotation speed could have a more consolidated structure which causes a lower strain. For Alg/SF wheel spun fibers, the mechanical properties are totally opposite. Thus, we assume the Alg/SF, a heterogeneous matter, would become more unconsolidated. These unconsolidated structures are beneficial to the VEGF quick release. This is the reason why the 60 rpm specimens, especially for Alg/SF groups, were selected for further VEGF loading and releasing study in this work. Two different morphologies of SF were applied to further control the VEGF releasing, degradation, mechanical behavior of Alg/SF fibers.

However, the influence of the rotation speed is significantly less important than the influence from the fiber themselves, i.e., spinning concentration and silk fibroin morphologies. Combining with the demonstrated SEM and XRD data, as well as the previously established alginate aggregation theory [21], it could be confirmed the three kinds of fibers are under low crystallinity and low orientation states. This may be due to the soft drafting effect of wheel spinning on the fiber, along with the relatively low temperature and low ions concentration. All these conditions of force, temperature, and solvent avoid the induced re-crystallization. The relatively low crystallinity and low orientation fiber is conducive to the VEGF quick release.

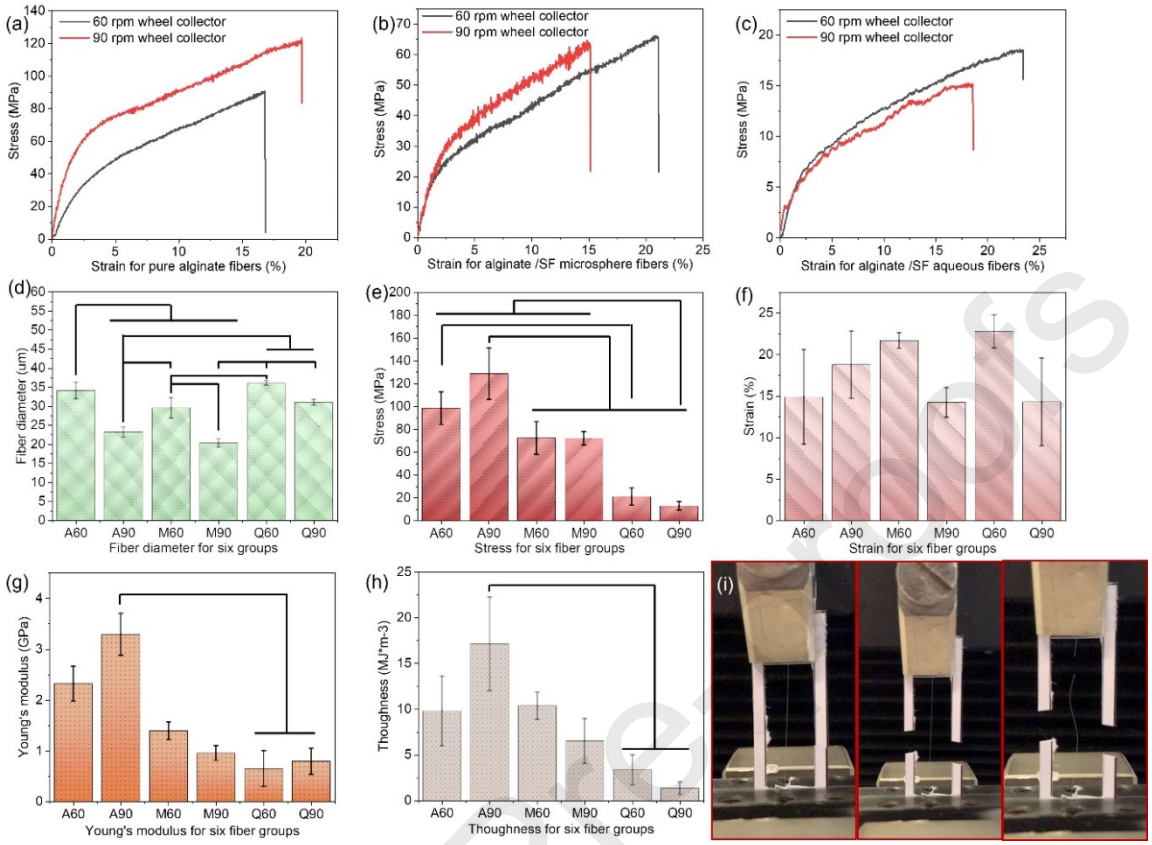

Figure 7. (a-c) stress-strain curves of pure alginate or Alg/SF wheel spun fibers. (d) fiber diameter counts of pure alginate or Alg/SF wheel spun fibers. (e-h) stress, strain, Young's modulus, and toughness of pure alginate or Alg/SF wheel spun fibers. (i) the optical images of tensile test for Alg/SF fibers.

4. Conclusion

In summary, Alg/SF composite fibers loaded with VEGF were successfully fabricated by using a new wheel spinning technique which parameters were optimized. We have demonstrated that the release of VEGF is controllable by engineering the Alg/SF composite fibers with different loading concentration and SF materials with different structure features. The mechanisms and impacting factors for VEGF release behavior from SF morphology and spinning solution concentration have been identified by analyzing the DoE results, indicating that Alg/SF composite fibers with different VEGF release rates could be utilized to develop new approaches to control the wound healing process.

Declaration of competing interest

The authors declare that they have no known competing financial interests or personal relationships that could have appeared to influence the study reported in this article.

Supporting Information

The Supporting Information is available free of charge at XXXXXX

Author Contributions

Jun Song and **Zhongda Chen** contributed equally to this work. All authors have read and approved the final manuscript.

Acknowledgments

Zhongda Chen and Jun Song acknowledge Mr. Luis Larrea Murillo who did the cell work of this project and financially supported by EPSRC & MRC Centre for Doctoral Training (CDT) program in the Division of Evolution and Genomic Sciences, The University of Manchester. The authors would like to express thanks to the support from Dr. Louise Carney and the Electron Microscopy Center and XRD suite in Department of Materials, The University of Manchester. SPSS, Minitab, and MATLAB were used under the license in The University of Manchester.

References

[1] P. Martin, R. Nunan, Cellular and molecular mechanisms of repair in acute and chronic wound healing, Br. J. Dermatol. 173 (2015) 370–378. https://doi.org/10.1111/bjd.13954.

[2] S. WERNER, R. GROSE, Regulation of Wound Healing by Growth Factors and Cytokines, Physiol. Rev. 83 (2003) 835–870. https://doi.org/10.1152/physrev.2003.83.3.835.

[3] J.S. Boateng, K.H. Matthews, H.N.E. Stevens, G.M. Eccleston, Wound Healing Dressings and Drug Delivery Systems: A Review, J. Pharm. Sci. 97 (2008) 2892–2923. https://doi.org/10.1002/jps.21210.

[4] P. Martin, Wound Healing--Aiming for Perfect Skin Regeneration, Science (80-.). 276 (1997) 75–81. https://doi.org/10.1126/science.276.5309.75.

[5] A.J. Rufaihah, N.A. Johari, S.R. Vaibavi, M. Plotkin, D.T. Di Thien, T. Kofidis, D. Seliktar, Dual delivery of VEGF and ANG-1 in ischemic hearts using an injectable hydrogel, Acta Biomater. 48 (2017) 58–67. https://doi.org/10.1016/j.actbio.2016.10.013.

[6] N. Kamaly, B. Yameen, J. Wu, O.C. Farokhzad, Degradable Controlled-Release Polymers and Polymeric Nanoparticles: Mechanisms of Controlling Drug Release, Chem. Rev. 116 (2016) 2602–2663. https://doi.org/10.1021/acs.chemrev.5b00346.

[7] W. Xu, Q. Song, J.-F. Xu, M.J. Serpe, X. Zhang, Supramolecular Hydrogels Fabricated from Supramonomers: A Novel Wound Dressing Material, ACS Appl. Mater. Interfaces. 9 (2017) 11368–11372. https://doi.org/10.1021/acsami.7b02850.

[8] X. Qiu, J. Zhang, L. Cao, Q. Jiao, J. Zhou, L. Yang, H. Zhang, Y. Wei, Antifouling Antioxidant Zwitterionic Dextran Hydrogels as Wound Dressing Materials with Excellent Healing Activities, ACS Appl. Mater. Interfaces. 13 (2021) 7060–7069. https://doi.org/10.1021/acsami.0c17744.

[9] M. Umar, A. Ullah, H. Nawaz, T. Areeb, M. Hashmi, D. Kharaghani, K.O. Kim, I.S. Kim, Wet-spun bi-component alginate based hydrogel fibers: Development and in-vitro evaluation as a potential moist wound care dressing, Int. J. Biol. Macromol. 168 (2021)

601–610. https://doi.org/10.1016/j.ijbiomac.2020.12.088.

[10] A. Vijayan, S. A., G.S.V. Kumar, PEG grafted chitosan scaffold for dual growth factor delivery for enhanced wound healing, Sci. Rep. 9 (2019) 19165. https://doi.org/10.1038/s41598-019-55214-7.

[11] J. Xia, H. Zhang, F. Yu, Y. Pei, X. Luo, Superclear, Porous Cellulose Membranes with Chitosan-Coated Nanofibers for Visualized Cutaneous Wound Healing Dressing, ACS Appl. Mater. Interfaces. 12 (2020) 24370–24379. https://doi.org/10.1021/acsami.0c05604.

[12] J. Hu, S. Chen, A review of actively moving polymers in textile applications, J. Mater. Chem. 20 (2010) 3346. https://doi.org/10.1039/b922872a.

[13] A. Joshi, Z. Xu, Y. Ikegami, K. Yoshida, Y. Sakai, A. Joshi, T. Kaur, Y. Nakao, Y. Yamashita, H. Baba, S. Aishima, N. Singh, H. Ijima, Exploiting synergistic effect of externally loaded bFGF and endogenous growth factors for accelerated wound healing using heparin functionalized PCL/gelatin co-spun nanofibrous patches, Chem. Eng. J. 404 (2021) 126518. https://doi.org/10.1016/j.cej.2020.126518.

[14] D.P. Tong, Process for the production of alginate fibre material and products made therefrom, US4562110A, 1985. https://patents.google.com/patent/US4562110A/en.

[15] Y.-M. Xia, Z.-D. Chen, Y. Li, Mechanical Properties Tests of Wet-spun Pure Alginate Filament and Yarns, in: Text. Bioeng. Informatics Symp. Proc. 2018 - 11th Text. Bioeng. Informatics Symp. TBIS 2018, 2018: pp. 37–46.

[16] Y. Luo, Y. Li, X. Qin, Q. Wa, 3D printing of concentrated alginate/gelatin scaffolds with homogeneous nano apatite coating for bone tissue engineering, Mater. Des. 146 (2018) 12–19. https://doi.org/10.1016/j.matdes.2018.03.002.

[17] L.-B. Jiang, S.-L. Ding, W. Ding, D.-H. Su, F.-X. Zhang, T.-W. Zhang, X.-F. Yin, L. Xiao, Y.-L. Li, F.-L. Yuan, J. Dong, Injectable sericin based nanocomposite hydrogel for multi-modal imaging-guided immunomodulatory bone regeneration, Chem. Eng. J. 418 (2021) 129323. https://doi.org/10.1016/j.cej.2021.129323.

[18] Z. Cao, X. Chen, J. Yao, L. Huang, Z. Shao, The preparation of regenerated silk fibroin microspheres, Soft Matter. 3 (2007) 910. https://doi.org/10.1039/b703139d.

[19] J. Song, X.-Q. Wang, J.-S. Li, Preparation of the silk fibroin 3D scaffolds with large pore sizes and high interconnectivity, in: Text. Bioeng. Informatics Symp. Proc. 2018 - 11th Text. Bioeng. Informatics Symp. TBIS 2018, 2018.

[20] J. Song, Z. Chen, L.L. Murillo, D. Tang, C. Meng, X. Zhong, T. Wang, J. Li, Hierarchical porous silk fibroin/poly(L-lactic acid) fibrous membranes towards vascular scaffolds, Int. J. Biol. Macromol. 166 (2021) 1111–1120. https://doi.org/10.1016/j.ijbiomac.2020.10.266.

[21] Z. Chen, J. Song, Y. Xia, Y. Jiang, L.L. Murillo, O. Tsigkou, T. Wang, Y. Li, High strength and strain alginate fibers by a novel wheel spinning technique for knitting stretchable and biocompatible wound-care materials, Mater. Sci. Eng. C. 127 (2021) 112204. https://doi.org/10.1016/j.msec.2021.112204.

[22] N. Sarlak, M.A.F. Nejad, S. Shakhesi, K. Shabani, Effects of electrospinning parameters on titanium dioxide nanofibers diameter and morphology: An investigation by Box–

Wilson central composite design (CCD), Chem. Eng. J. 210 (2012) 410–416. https://doi.org/10.1016/j.cej.2012.08.087.

[23] D.N. Rockwood, R.C. Preda, T. Yücel, X. Wang, M.L. Lovett, D.L. Kaplan, Materials fabrication from Bombyx mori silk fibroin, Nat. Protoc. 6 (2011) 1612–1631. https://doi.org/10.1038/nprot.2011.379.

[24] T. Asakura, K. Ohgo, T. Ishida, P. Taddei, P. Monti, R. Kishore, Possible Implications of Serine and Tyrosine Residues and Intermolecular Interactions on the Appearance of Silk I Structure of Bombyx m ori Silk Fibroin-Derived Synthetic Peptides: High-Resolution 13 C Cross-Polarization/Magic-Angle Spinning NMR Study, Biomacromolecules. 6 (2005) 468–474. https://doi.org/10.1021/bm049487k.

[25] J. Yan, G. Zhou, D.P. Knight, Z. Shao, X. Chen, Wet-Spinning of Regenerated Silk Fiber from Aqueous Silk Fibroin Solution: Discussion of Spinning Parameters, Biomacromolecules. 11 (2010) 1–5. https://doi.org/10.1021/bm900840h.

[26] D.M. Phillips, L.F. Drummy, R.R. Naik, H.C. De Long, D.M. Fox, P.C. Trulove, R.A. Mantz, Regenerated silk fiber wet spinning from an ionic liquid solution, J. Mater. Chem. 15 (2005) 4206. https://doi.org/10.1039/b510069k.

[27] F. Zhang, Q. Lu, X. Yue, B. Zuo, M. Qin, F. Li, D.L. Kaplan, X. Zhang, Regeneration of high-quality silk fibroin fiber by wet spinning from CaCl 2 –formic acid solvent, Acta Biomater. 12 (2015) 139–145. https://doi.org/10.1016/j.actbio.2014.09.045.

[28] Q. Liu, K.K. Parker, A viscoelastic beam theory of polymer jets with application to rotary jet spinning, Extrem. Mech. Lett. 25 (2018) 37–44. https://doi.org/10.1016/j.eml.2018.10.005.

[29] L.W. Schwartz, R.V. Roy, Theoretical and numerical results for spin coating of viscous liquids, Phys. Fluids. 16 (2004) 569–584. https://doi.org/10.1063/1.1637353.

[30] Y. Wu, C. Li, F. Fan, J. Liang, Z. Yang, X. Wei, S. Chen, PVAm Nanofibers Fabricated by Rotary Jet Wet Spinning and Applied to Bisphenol A Recognition, ACS Omega. 4 (2019) 21361–21369. https://doi.org/10.1021/acsomega.9b02964.

[31] W. Mackie, S. Perez, R. Rizzo, F. Taravel, M. Vignon, Aspects of the conformation of polyguluronate in the solid state and in solution, Int. J. Biol. Macromol. 5 (1983) 329–341. https://doi.org/10.1016/0141-8130(83)90056-9.

[32] M.B. Stewart, S.R. Gray, T. Vasiljevic, J.D. Orbell, The role of poly-M and poly-GM sequences in the metal-mediated assembly of alginate gels, Carbohydr. Polym. 112 (2014) 486–493. https://doi.org/10.1016/j.carbpol.2014.06.001.

[33] M. Farokhi, F. Mottaghitalab, Y. Fatahi, A. Khademhosseini, D.L. Kaplan, Overview of Silk Fibroin Use in Wound Dressings, Trends Biotechnol. 36 (2018) 907–922. https://doi.org/10.1016/j.tibtech.2018.04.004.

[34] W. Chen, F. Li, L. Chen, Y. Zhang, T. Zhang, T. Wang, Fast self-assembly of microporous silk fibroin membranes on liquid surface, Int. J. Biol. Macromol. 156 (2020) 633–639. https://doi.org/https://doi.org/10.1016/j.ijbiomac.2020.04.053.

[35] B. Liu, B.Z. Tang, Aggregation-Induced Emission: More Is Different, Angew. Chemie Int. Ed. 59 (2020) 9788–9789. https://doi.org/10.1002/anie.202005345.

[36] P.F. Ng, K.I. Lee, S. Meng, J. Zhang, Y. Wang, B. Fei, Wet Spinning of Silk Fibroin-Based Core–Sheath Fibers, ACS Biomater. Sci. Eng. 5 (2019) 3119–3130. https://doi.org/10.1021/acsbiomaterials.9b00275.

[37] G. Song, C. Zheng, Y. Liu, M. Ding, P. Liu, J. Xu, W. Wang, J. Wang, In vitro extracellular matrix deposition by vascular smooth muscle cells grown in fibroin scaffolds, and the regulation of TGF-β1, Mater. Des. 199 (2021) 109428. https://doi.org/10.1016/j.matdes.2020.109428.

[38] N. Yin, Y. Han, H. Xu, Y. Gao, T. Yi, J. Yao, L. Dong, D. Cheng, Z. Chen, VEGF-conjugated alginate hydrogel prompt angiogenesis and improve pancreatic islet engraftment and function in type 1 diabetes, Mater. Sci. Eng. C. 59 (2016) 958–964. https://doi.org/10.1016/j.msec.2015.11.009.

[39] Y. Zhang, J. Huang, L. Huang, Q. Liu, H. Shao, X. Hu, L. Song, Silk Fibroin-Based Scaffolds with Controlled Delivery Order of VEGF and BDNF for Cavernous Nerve Regeneration, ACS Biomater. Sci. Eng. 2 (2016) 2018–2025. https://doi.org/10.1021/acsbiomaterials.6b00436.

[40] N. Hassani Besheli, S. Damoogh, B. Zafar, F. Mottaghitalab, H. Motasadizadeh, F. Rezaei, M.A. Shokrgozar, M. Farokhi, Preparation of a Codelivery System Based on Vancomycin/Silk Scaffold Containing Silk Nanoparticle Loaded VEGF, ACS Biomater. Sci. Eng. 4 (2018) 2836–2846. https://doi.org/10.1021/acsbiomaterials.8b00149.

[41] M. Farokhi, F. Mottaghitalab, M.A. Shokrgozar, J. Ai, J. Hadjati, M. Azami, Bio-hybrid silk fibroin/calcium phosphate/PLGA nanocomposite scaffold to control the delivery of vascular endothelial growth factor, Mater. Sci. Eng. C. 35 (2014) 401–410. https://doi.org/10.1016/j.msec.2013.11.023.

[42] Y. Wu, T. Chang, W. Chen, X. Wang, J. Li, Y. Chen, Y. Yu, Z. Shen, Q. Yu, Y. Zhang, Release of VEGF and BMP9 from injectable alginate based composite hydrogel for treatment of myocardial infarction, Bioact. Mater. 6 (2021) 520–528. https://doi.org/10.1016/j.bioactmat.2020.08.031.

[43] G. Marchioli, A. Di Luca, E. de Koning, M. Engelse, C.A. Van Blitterswijk, M. Karperien, A.A. Van Apeldoorn, L. Moroni, Hybrid Polycaprolactone/Alginate Scaffolds Functionalized with VEGF to Promote de Novo Vessel Formation for the Transplantation of Islets of Langerhans, Adv. Healthc. Mater. 5 (2016) 1606–1616. https://doi.org/10.1002/adhm.201600058.

[44] R. Zhang, L. Xie, H. Wu, T. Yang, Q. Zhang, Y. Tian, Y. Liu, X. Han, W. Guo, M. He, S. Liu, W. Tian, Alginate/laponite hydrogel microspheres co-encapsulating dental pulp stem cells and VEGF for endodontic regeneration, Acta Biomater. 113 (2020) 305–316. https://doi.org/10.1016/j.actbio.2020.07.012.

[45] A.M. Craciun, L. Mititelu Tartau, M. Pinteala, L. Marin, Nitrosalicyl-imine-chitosan hydrogels based drug delivery systems for long term sustained release in local therapy, J. Colloid Interface Sci. 536 (2019) 196–207. https://doi.org/10.1016/j.jcis.2018.10.048.

[46] D. Ailincai, M. Agop, I.C. Marinas, A. Zala, S.A. Irimiciuc, L. Dobreci, T.-C. Petrescu, C. Volovat, Theoretical model for the diclofenac release from PEGylated chitosan hydrogels,

Drug Deliv. 28 (2021) 261–271. https://doi.org/10.1080/10717544.2021.1876181.

[47] J.F. Dye, From Secondary Intent to Accelerated Regenerative Healing: Emergence of the Bio-intelligent Scaffold Vasculogenic Strategy for Skin Reconstruction, in: Vasc. Tissue Eng. Regen. Med., Springer International Publishing, Cham, 2020: pp. 1–68. https://doi.org/10.1007/978-3-319-21056-8_20-1.

[48] C. Chen, Y. Wang, D. Zhang, X. Wu, Y. Zhao, L. Shang, J. Ren, Y. Zhao, Natural polysaccharide based complex drug delivery system from microfluidic electrospray for wound healing, Appl. Mater. Today. 23 (2021) 101000. https://doi.org/10.1016/j.apmt.2021.101000.

[49] Y. Guo, J. Guan, H. Peng, X. Shu, L. Chen, H. Guo, Tightly adhered silk fibroin coatings on Ti6Al4V biometals for improved wettability and compatible mechanical properties, Mater. Des. 175 (2019) 107825. https://doi.org/10.1016/j.matdes.2019.107825.

CRediT authorship contribution statement:

Jun Song and **Zhongda Chen** contributed equally to this work.

Jun Song: Methodology, Visualization, Investigation and Writing - review & editing.

Zhongda Chen: Project administration, Conceptualization, Methodology, Investigation, Data curation and Writing - original draft.

Zekun Liu: Methodology, Investigation.

Yangpeiqi Yi: Investigation, Data curation.

Olga Tsigkou: Methodology, Investigation.

Jiashen Li: Supervision, Methodology.

Yi Li: Project administration, Conceptualization, Supervision, Data curation, Writing - review & editing.